

风蚀与植被耦合的离散动力学模型研究

吴选文, 张化永*, 黄头生

华北电力大学, 北京

Email: 13520899951@163.com, *50902253@ncepu.edu.cn, rceens@ncepu.edu.cn

收稿日期: 2021年2月16日; 录用日期: 2021年3月11日; 发布日期: 2021年3月19日

摘要

为了探究风蚀和植被的系统动力学, 本文构建了一个离散的风蚀-植被动力学模型, 并通过平衡点的稳定性分析以及分岔分析, 得到了系统产生Neimark-Sacker分岔的条件。通过数值模拟, 展示了由Neimark-Sacker分岔引起的复杂动力学行为, 这些行为能为风蚀-植被系统的复杂动态变化提供解释。

关键词

动力学, 平衡点, Neimark-Sacker分岔

Research on Discrete Dynamical Model Coupled by Wind Erosion and Vegetation

Xuanwen Wu, Huayong Zhang*, Tousheng Huang

North China Electric Power University, Beijing

Email: 13520899951@163.com, *50902253@ncepu.edu.cn, rceens@ncepu.edu.cn

Received: Feb. 16th, 2021; accepted: Mar. 11th, 2021; published: Mar. 19th, 2021

Abstract

In order to explore the system dynamics of wind erosion and vegetation, this research constructs a discrete erosion-vegetation dynamical model. Through stability analysis of equilibriums and bifurcation analysis, the conditions for the system to produce the Neimark-Sacker bifurcation are obtained. Numerical simulations show the complex dynamical behaviors induced by the Neimark-Sacker bifurcation, which can provide an explanation for the complex dynamic changes of the erosion-vegetation system.

*通讯作者。

Keywords

Dynamics, Equilibrium, Neimark-Sacker Bifurcation

Copyright © 2021 by author(s) and Hans Publishers Inc.

This work is licensed under the Creative Commons Attribution International License (CC BY 4.0).

<http://creativecommons.org/licenses/by/4.0/>



Open Access

1. 引言

风蚀是侵蚀生态系统中的一种驱动因素。为了研究侵蚀生态系统中风蚀的动力学机制，本文建立了风蚀 - 植被动力学方程。研究表明，时间离散的系统会产生 Neimark-Sacker 分岔，并且进一步能形成周期环、倍周期分岔等非线性过程[1] [2] [3]。动力学分析是探究系统分岔方式的常用手段，基于理论进行分岔分析，并结合数值模拟可以得到系统的分岔图与相位图。分岔图与相位图能够直观展现风蚀 - 植被系统中 Neimark-Sacker 分岔引起的各种动力学过程。

2. 模型构建与分岔分析

在地表风力侵蚀过程中，植被的存在可以减弱风力强度。并且植被的根茎部分能够增强土壤的凝聚力从而减小风力对地表的剥蚀[4]。在风蚀地区，植被与沉积沙的相互作用关系复杂。本文将植被对沉积沙的影响分为两个部分。1) 植被的阻沙作用：植物的繁茂枝叶对风沙流中的沙粒具有拦截作用。植被的存在使得风成沙的沉积率增加[5] [6]。2) 植被的固沙作用：改变了沙表性质，使其起动风速阈值大于当地最大风速值等条件。同样的，空气中的沙子沉积到植被所覆盖的区域后，也会对植被的生长产生影响。例如，风力对地表的剥蚀作用可以给植物带来生长所需的无机营养物质。从这方面上讲，风蚀的分离作用会对植被起到一定的促进作用。另一方面，沉积沙的增加对植被有一定的掩埋作用，则植物就需要进一步的生长以裸露出足够多的部分，以保证地面部分进行光合作用。风力侵蚀分为风蚀、搬运和沉积过程，这三个过程对植被均有不同的作用影响。

根据植被 - 沉积沙相互作用关系与先前的研究工作[7] [8]，将植被的覆盖度和沉积沙的高度作为状态变量，得到了离散的风蚀 - 植被动力学模型映射关系：

$$\begin{pmatrix} s \\ v \end{pmatrix} \rightarrow \begin{pmatrix} s + t \left(\frac{k_m (V + k_0 D)}{\varepsilon (V + k_m D)} - \frac{a S e^{-bv}}{\varepsilon} \right) \\ v + thV \left(1 - \frac{V}{V_m} - \frac{cS}{f + V} - g \frac{\partial S}{\partial t} \right) \end{pmatrix} \quad (1)$$

其中， k_m ：最大植被覆盖度下沉积沙沉积速率(cm year^{-1})； D ：植被对沉积沙的影响系数($\text{cm}^{-1} \text{ year}$)； a ：沉积沙对自身高度的抑制系数(year^{-1})； b ：植被对沉积沙的固定作用系数(cm^{-1})； g ：沉积沙高度变化对植被生长的抑制系数(month cm^{-1})；

本文中依据 Guckenheimer 和 Holmes [9]述的 Neimark-Sacker 分岔定理，解得系统(1)的两个平衡点分别为 $E_0 \left(\frac{k_0}{a}, 0 \right)$ ， $E_1 (s_1, v_1)$ 。因此，映射(1)在点 (s, v) 所对应的雅克比矩阵为：

$$J = \begin{pmatrix} J_{11} & J_{12} \\ J_{13} & J_{14} \end{pmatrix} \quad (2)$$

其中

$$\begin{aligned} J_{11} &= \frac{\partial F}{\partial S} \Big|_{S_1, V_1}, J_{12} = \frac{\partial F}{\partial V} \Big|_{S_1, V_1} \\ J_{21} &= \frac{\partial G}{\partial S} \Big|_{S_1, V_1}, J_{22} = \frac{\partial G}{\partial V} \Big|_{S_1, V_1} \end{aligned} \tag{3}$$

$$F(S, V) = s + \frac{t}{\varepsilon} \left(\frac{k_m(V + k_0 D)}{V + k_m D} - a S e^{-bV} \right), F(S_1, V_1) = 0 \tag{4}$$

$$G(S, V) = v + t h V \left(1 - \frac{V}{V_m} - \frac{cS}{f + V} - g \frac{\partial S}{\partial t} \right), G(S_1, V_1) = 0$$

将 $E_0 \left(\frac{k_0}{a}, 0 \right)$ 代入方程(2)可得:

$$J_0 = \begin{pmatrix} 1 - \frac{at}{\varepsilon} & t \left(\frac{k_m - k_0}{\varepsilon k_2 D} + \frac{k_0 b}{\varepsilon} \right) \\ 0 & 1 \end{pmatrix} \tag{5}$$

在给均匀定态解 $E_1(s_1, v_1)$ 加入微扰后, 将 $E_1(s_1, v_1)$ 代入雅可比矩阵可得:

$$J_1 = \begin{pmatrix} 1 + ta_{11} & ta_{12} \\ ta_{21} - tghv_1(1 + ta_{11}) & 1 + t(a_{22} - tghv_1 a_{12}) \end{pmatrix} \tag{6}$$

其中

$$\begin{aligned} a_{11} &= -\frac{k_m v_1 + k_0 D}{\varepsilon s_1 v_1 + k_m D}, a_{12} = \frac{k_2 D(k_m - k_0)}{\varepsilon (v_1 + k_m D)^2} + \frac{k_m b v_1 + k_0 D}{\varepsilon v_1 + k_m D} \\ a_{21} &= \frac{-chv_1}{f + v_1}, a_{22} = hv_1 \frac{V_m - f - 2v_1}{V_m (f + v_1)} \end{aligned} \tag{7}$$

结合上述方程, 我们分别可以得到雅可比矩阵 J_1 的迹和行列式:

$$\begin{aligned} tr(J_1) &= 2 + tp \\ \Delta(J_1) &= 1 + tp + t^2 q \\ p &= a_{11} + a_{22} - tghv_1 a_{12} \\ q &= a_{11} a_{22} - a_{12} a_{21} + ghv_1 a_{12} \end{aligned} \tag{8}$$

从而解得对应的雅可比矩阵的特征值:

$$\lambda_{1,2} = \frac{tr \pm \sqrt{tr^2 - 4\Delta}}{2} \tag{9}$$

Neimark-Sacker 分岔条件之一是方程(9)的特征值为一对模为 1 的共轭复数[10]。这就要求: $tr^2 - 4\Delta$, 且 $\Delta = 1$ 。解得

$$h_{ns} = -\frac{a_{11}}{t(a_{11} A_{22} - A_{21} a_{12}) + A_{22}} \tag{10}$$

其中 $A_{21} = \frac{-cv_1}{f + v_1}$, $A_{22} = v_1 \frac{V_m - f - 2v_1}{V_m (f + v_1)}$ 。

然后通过下式将均匀定态平衡点 $E_1(s_1, v_1)$ 平移至原点, 令

$$x = s - s_1, \quad y = v - v_1 \tag{11}$$

将式子(11)代入式子(2)中, 经泰勒展开可以得到如下映射,

$$\begin{pmatrix} x \\ y \end{pmatrix} \rightarrow \begin{pmatrix} d_{11}x + d_{12}y + d_{13}y^2 + d_{14}xy + d_{15}xy^2 + d_{16}y^3 + O\left(\left(|x| + |y|\right)^4\right) \\ d_{21}x + d_{22}y + d_{23}y^2 + d_{24}xy + d_{25}xy^2 + d_{26}y^3 + O\left(\left(|x| + |y|\right)^4\right) \end{pmatrix} \tag{12}$$

其中

$$\begin{aligned} d_{11} &= 1 + ta_{11}, \quad d_{12} = ta_{12}, \\ d_{13} &= -\frac{t}{\varepsilon} \left(\frac{k_m D(k_m - k_0)}{(v_1 + k_m D)^3} + ab^2 s_1 e^{-bv_1} \right), \quad d_{14} = \frac{tab}{\varepsilon} e^{-bv_1}, \\ d_{15} &= -\frac{tab^2}{\varepsilon} e^{-bv_1}, \quad d_{16} = \frac{t}{\varepsilon} \left(\frac{k_2 D(k_2 - k_1)}{(v_1 + k_2 D)^4} + ab^3 s_1 e^{-bv_1} \right), \\ d_{21} &= ta_{21} - tghv_1(1 + ta_{11}), \quad d_{22} = 1 + t(a_{22} - tghv_1 a_{12}), \\ d_{23} &= \frac{thcfs_1}{(f + v_1)^3} - \frac{th}{V_m} - thg(d_{12} + v_1 d_{12}), \\ d_{24} &= -thg(d_{11} + v_1 d_{14}) - \frac{thcf}{(f + v_1)^2}, \\ d_{25} &= -thg(d_{14} + v_1 d_{15}) + \frac{thcf}{(f + v_1)^3}, \\ d_{26} &= -thg(d_{13} + v_1 d_{16}) - \frac{thcfs_1}{(f + v_1)^4} \end{aligned} \tag{13}$$

Neimark-Sacker 分岔的第二个条件是

$$\mu = \left. \frac{d|\lambda|}{dh} \right|_{h=h_0} \neq 0, \quad (\lambda(h))^n \neq 1, \quad n = 1, 2, 3, 4 \tag{14}$$

$$\lambda(h) = \frac{tr(h) \pm i\sqrt{4\Delta(h) - tr(h)^2}}{2} = \alpha \pm i\beta, \quad i = \sqrt{-1} \tag{15}$$

方程(14)等价于式子(8)中的 $tr \neq -2, -1, 0, 2$ 。由于在方程(9)中 $tr^2 \neq 4$, 则进一步改写条件为 $tr \neq -1, 0$, 即

$$t(a_{11} + a_{22} - tghv_1 a_{12}) \neq -3, -2 \tag{16}$$

再基于映射(12)的规范型进行 Neimark-Sacker 分岔分析, 应用可逆变换:

$$\begin{pmatrix} x \\ y \end{pmatrix} = \begin{pmatrix} d_{12} & 0 \\ \alpha - d_{11} & -\beta \end{pmatrix} \begin{pmatrix} \bar{x} \\ \bar{y} \end{pmatrix} \tag{17}$$

代入映射(12)后得,

$$\begin{pmatrix} \bar{x} \\ \bar{y} \end{pmatrix} \rightarrow \begin{pmatrix} \alpha & -\beta \\ \beta & \alpha \end{pmatrix} \begin{pmatrix} \bar{x} \\ \bar{y} \end{pmatrix} + \frac{1}{d_{12}\alpha} \begin{pmatrix} M(\bar{x}, \bar{y}) \\ N(\bar{x}, \bar{y}) \end{pmatrix} \tag{18}$$

其中

$$\begin{aligned} M(\bar{x}, \bar{y}) &= \beta d_{13} \bar{y}^2 + \beta d_{14} \bar{x} \bar{y} + \beta d_{15} \bar{x} \bar{y}^2 + \beta d_{16} \bar{y}^3 + O\left(\left(|\bar{x}| + |\bar{y}|\right)^4\right) \\ N(\bar{x}, \bar{y}) &= [(\alpha - d_{11})d_{13} - d_{12}d_{23}] \bar{y}^2 + [(\alpha - d_{11})d_{14} - d_{12}d_{24}] \bar{x} \bar{y} \\ &\quad + [(\alpha - d_{11})d_{15} - d_{12}d_{25}] \bar{x} \bar{y}^2 + [(\alpha - d_{11})d_{16} - d_{12}d_{26}] \bar{y}^3 + O\left(\left(|\bar{x}| + |\bar{y}|\right)^4\right) \end{aligned} \tag{19}$$

当条件(19)被满足时[11], 系统(17)在点(0, 0)处产生 Neimark-Sacker 分岔。

$$= -Re\left(\frac{(1-2\bar{\lambda})\bar{\lambda}^2}{1-\lambda} \xi_{11}\xi_{20}\right) - \frac{1}{2}|\xi_{11}|^2 - |\xi_{02}|^2 + Re(\bar{\lambda}\xi_{21}) \neq 0 \tag{20}$$

其中

$$\begin{aligned} \xi_{20} &= \frac{1}{8}\left((M_{\bar{x}\bar{x}} - M_{\bar{y}\bar{y}} + 2N_{\bar{x}\bar{y}}) + i(N_{\bar{x}\bar{x}} - N_{\bar{y}\bar{y}} - 2M_{\bar{x}\bar{y}})\right) \\ \xi_{11} &= \frac{1}{4}\left((M_{\bar{x}\bar{x}} + M_{\bar{y}\bar{y}}) + i(N_{\bar{x}\bar{x}} + N_{\bar{y}\bar{y}})\right) \\ \xi_{02} &= \frac{1}{8}\left((M_{\bar{x}\bar{x}} - M_{\bar{y}\bar{y}} - 2N_{\bar{x}\bar{y}}) + i(N_{\bar{x}\bar{x}} - N_{\bar{y}\bar{y}} + 2M_{\bar{x}\bar{y}})\right) \\ \xi_{21} &= \frac{1}{16}\left((M_{\bar{x}\bar{x}\bar{x}} + M_{\bar{y}\bar{y}\bar{y}} + N_{\bar{x}\bar{y}\bar{y}} + N_{\bar{y}\bar{y}\bar{y}}) + i(N_{\bar{x}\bar{x}\bar{x}} + N_{\bar{y}\bar{y}\bar{y}} - M_{\bar{x}\bar{y}\bar{y}} - M_{\bar{y}\bar{y}\bar{y}})\right) \end{aligned} \tag{21}$$

且 $M(\bar{x}, \bar{y})$ 和 $N(\bar{x}, \bar{y})$ 在 $\bar{x} = 0, \bar{y} = 0$ 处的二阶偏导数与三阶偏导数为:

$$\begin{aligned} M_{\bar{x}\bar{x}} &= \beta d_{13} (\alpha - d_{11})^2 + \beta d_{12} d_{14} (\alpha - d_{11}), \quad M_{\bar{y}\bar{y}} = \beta^3 d_{13}, \\ M_{\bar{x}\bar{y}} &= -\beta^2 (d_{12} d_{14} + 2d_{13} (\alpha - d_{11})), \\ N_{\bar{x}\bar{x}} &= ((\alpha - d_{11})d_{13} - d_{12}d_{23})(\alpha - d_{11})^2 + d_{12} (\alpha - d_{11})d_{14} - d_{12}d_{24} (\alpha - d_{11}), \\ N_{\bar{y}\bar{y}} &= \beta^2 ((\alpha - d_{11})d_{13} - d_{12}d_{23}), \\ N_{\bar{x}\bar{y}} &= -\beta d_{12} ((\alpha - d_{11})d_{13} - d_{12}d_{23}) - 2\beta (\alpha - d_{11})((\alpha - d_{11})d_{14} - d_{12}d_{24}), \\ M_{\bar{x}\bar{x}\bar{x}} &= \beta (\alpha - d_{11})^2 (d_{12}d_{15} + d_{16} (\alpha - d_{11})), \\ M_{\bar{x}\bar{y}\bar{y}} &= -\beta^2 (\alpha - d_{11})(2d_{12}d_{15} + 3d_{16} (\alpha - d_{11})), \\ M_{\bar{y}\bar{y}\bar{y}} &= \beta^3 (d_{12}d_{15} + 3d_{16} (\alpha - d_{11})), \quad M_{\bar{y}\bar{y}\bar{y}} = -\beta^4 d_{16}, \\ N_{\bar{x}\bar{x}\bar{x}} &= (\alpha - d_{11})^2 (d_{12} ((\alpha - d_{11})d_{15} - d_{12}d_{25}) + ((\alpha - d_{11})d_{16} - d_{12}d_{26})(\alpha - d_{11})), \\ N_{\bar{x}\bar{y}\bar{y}} &= -\beta (\alpha - d_{11})(2d_{12} ((\alpha - d_{11})d_{15} - d_{12}d_{25}) + 3((\alpha - d_{11})d_{16} - d_{12}d_{26})(\alpha - d_{11})), \\ N_{\bar{y}\bar{y}\bar{y}} &= \beta^2 (d_{12} ((\alpha - d_{11})d_{15} - d_{12}d_{25}) + 3((\alpha - d_{11})d_{16} - d_{12}d_{26})(\alpha - d_{11})), \\ N_{\bar{y}\bar{y}\bar{y}} &= -\beta^3 ((\alpha - d_{11})d_{16} - d_{12}d_{26}) \end{aligned} \tag{22}$$

结合方程(19)、(20)、(21)，可以解得，

$$\begin{aligned}
 &= \frac{1}{K} \left\{ P \left(2M_{xx}N_{xx} + 2N_{xx}N_{yy} - 2N_{xy}N_{yy} - M_{yy}N_{xx} - M_{yy}N_{yy} \right) - 2PM_{xx}M_{xy} \right. \\
 &+ Q \left(N_{xx}^2 - N_{yy}^2 - M_{xx}^2 + N_{xx}M_{yy} - 2M_{xx}N_{xy} - 2M_{xy}N_{xx} - 2M_{xy}N_{yy} \right) \\
 &- \frac{1}{64d_{12}^2\beta^2} \left\{ 2M_{xx}^2 + 2(N_{xx} + N_{yy})^2 + (M_{xx} - 2N_{xy})^2 + (N_{xx} - N_{yy} + 2M_{xy})^2 \right\} \\
 &\left. + \frac{1}{16d_{12}\beta} \left\{ \alpha(M_{xxx} + N_{xxy}) + \beta(N_{xxx} + N_{xyy} - M_{xxy}) \right\} \right\} \neq 0 \tag{23}
 \end{aligned}$$

其中，

$$\begin{aligned}
 K &= 32d_{12}^2\beta^2 \left((1-\alpha)^2 + \beta^2 \right) \\
 M &= \beta(3-4\alpha)(\alpha^2 - \beta^2) - 2\alpha\beta \left((1-\alpha)(1-2\alpha) - 2\beta^2 \right) \\
 N &= (1-3\alpha + 2\alpha^2 - 2\beta^2)(\alpha^2 - \beta^2) + (6\alpha - 8\beta^2)\beta^2
 \end{aligned} \tag{24}$$

当条件(10)，(14)，(16)和(23)都被满足时，系统(1)在 $E_1(s_1, v_1)$ 处产生 Neimark-Sacker 分岔。如果式子(14)、(20)满足 $\eta < 0, \mu > 0$ ，产生的 Neimark-Sacker 分岔是超临界的，系统在平衡点 (s_1, v_1) 处失稳，进而导致系统中周期环的出现。

3. 数值模拟结果

在上一节内容中我们已经得到了系统的分岔条件，即当 $h = h_{ns}$ 时，系统达到临界点，当 $h > h_{ns}$ 时，系统发生 Neimark-Sacker 分岔。本节通过数值模拟展现参数变化时风蚀 - 植被系统的 Neimark-Sacker 分岔以及由分岔所引起的复杂动力学行为。当我们令参数值分别为 $k_0 = 5; k_m = 30; D = 0.1; a = 1; b = 0.04; V_m = 100; c = 0.5; f = 10; \varepsilon = 12; g = 0.01$ ，便可以得到如图 1 所示的特征值曲线图。红色曲线代表的是随着植被生长系数 h 的增大，系统从均匀稳定态过渡到不稳定状态的过程。

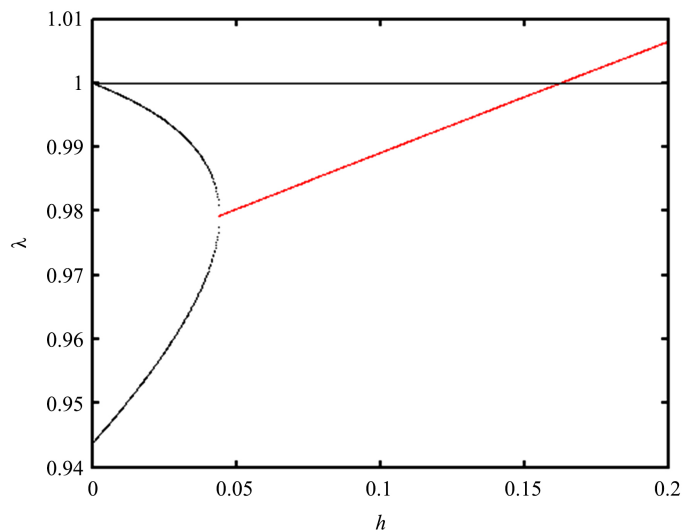


Figure 1. Eigenvalue curve graph
图 1. 特征值曲线图

在图 1 的基础上, 我们绘制了如图 2 所示的系统(1)随着参数 h 变化的分岔图。其中图 2(a)和图 2(c)分别为沉积沙与植被的分岔图, 图 2(b)和图 2(d)为与其对应的局部放大图, 展示了离散系统在趋于混沌过程中所产生的倍周期分岔过程。从图 2(a)和图 2(c)中可以看到, 当 $h < 0.1489$ 时, 沉积沙变量 S 与植被变量 V 处于渐进稳定状态。当系统越过临界点即 $h > 0.1489$ 时, 系统的稳定态消失, 并开始渐进不动点附近产生分岔。如图 2(b)和图 2(d)所示, 随着参数 h 的不断增大, 系统会经历倍周期分岔过程。

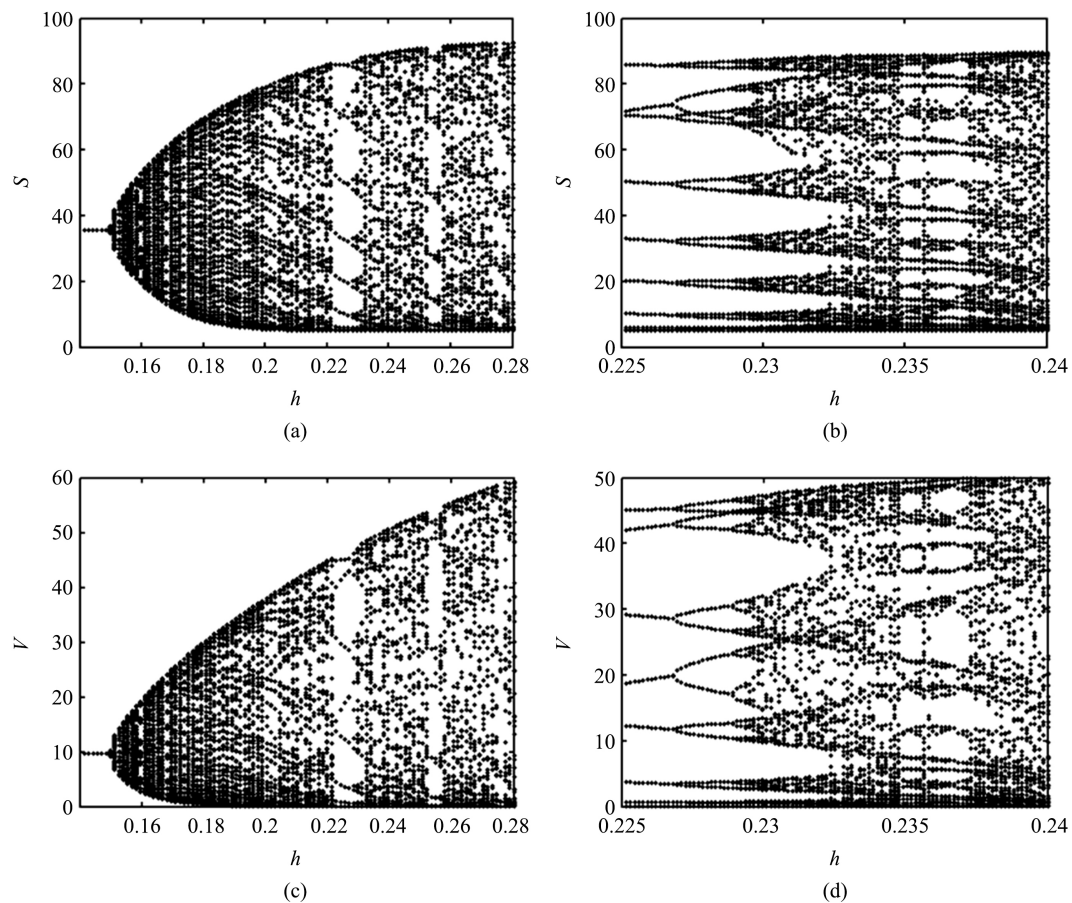


Figure 2. (a) and (c) are bifurcation diagrams, (b) and (d) are corresponding partial enlarged diagrams

图 2. (a)和(c)为分岔图, (b)和(d)为对应的局部放大图

为了更直观地观察在混沌路径上, 离散系统的吸引子是如何随着参数而发生改变的, 我们得到了如图 3 所示的相位图。图 3(a)与图 3(b)清晰地展示了系统从不动点到拟周期的转变过程。再随着参数 h 的增大, 又经历了不变环(图 3(c))以及倍周期过程(图 3(d))。

大量研究成果表明[12][13][14], 在离散动力学系统研究领域, Neimark-Sacker 分岔是最重要的分岔之一。本文在时间离散风蚀 - 植被模型中, 应用 Neimark-Sacker 分岔来探究植被与风成沙的复杂动力学机制。从图 3 可以观察到, 对于不同生长速率的植被而言, 存在与沙丘的动态平衡机制。风蚀地区的植被生长受当地气候影响, 在不同时期有着较大的区别, 这意味着风蚀 - 植被系统很难保持在稳定平衡状态。且从图 3 可以看到植被覆盖度越高, 沙丘则越大, 表明了植被覆盖促进了沙丘的增长与稳定存在。在本文中, 我们通过改变植被生长系数 h 的大小, 发现植被生长系数与沙丘的大小成正相关。动力学分析作为一种重要的研究方法, 其可以通过大量的数值模拟来展现出各个环境因素对整个系统的影响。

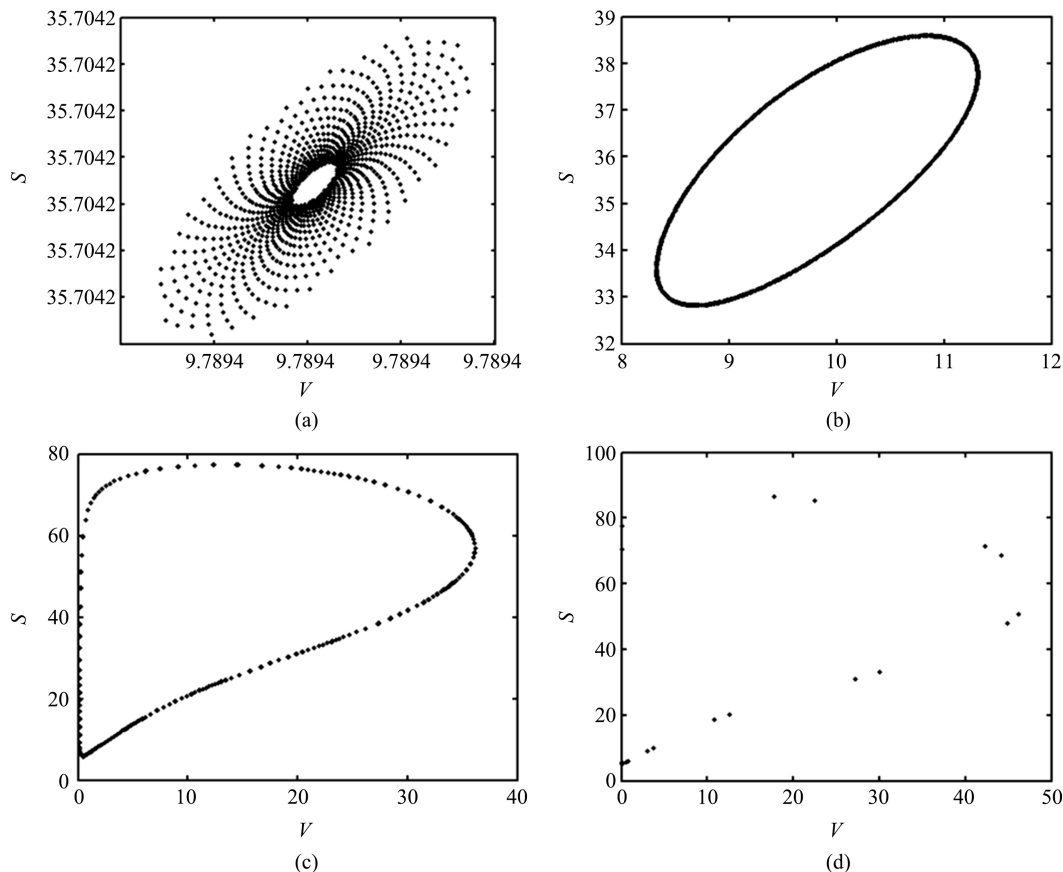


Figure 3. Phase diagram
 图 3. 相位图

基金项目

本研究受到国家水污染控制与治理科技重大专项(No. 2017ZX07101003-06)的资助与支持。

参考文献

- [1] Yuan, L.G. and Yang, Q.G. (2015) Bifurcation, Invariant Curve and Hybrid Control in a Discrete-Time Predator-Prey System. *Applied Mathematical Modelling*, **39**, 2345-2362. <https://doi.org/10.1016/j.apm.2014.10.040>
- [2] Jing, Z. and Yang, J. (2006) Bifurcation and Chaos in Discrete-Time Predator-Prey System. *Chaos Solitons & Fractals*, **27**, 259-277. <https://doi.org/10.1016/j.chaos.2005.03.040>
- [3] Liu, X. and Xiao, D. (2007) Complex Dynamic Behaviors of a Discrete-Time Predator-Prey System. *Chaos, Solitons & Fractals*, **32**, 80-94. <https://doi.org/10.1016/j.chaos.2005.10.081>
- [4] Hoonhout, B.M. and Vries, S. (2016) A Process-Based Model for Aeolian Sediment Transport and Spatiotemporal Varying Sediment Availability. *Journal of Geophysical Research: Earth Surface*, **121**, 1555-1575. <https://doi.org/10.1002/2015JF003692>
- [5] Eldridge, D.J. and Leys, J.F. (2003) Exploring Some Relationships between Biological Soil Crusts, Soil Aggregation and Wind Erosion. *Journal of arid Environments*, **53**, 457-466. <https://doi.org/10.1006/jare.2002.1068>
- [6] Namikas, S.L. and Sherman, D.J. (1995) A Review of the Effects of Surface Moisture Content on Aeolian sand Transport. In: Tchakerian, V.P. (Ed.), *Desert Aeolian Processes*, Springer, Dordrecht, 269-293. https://doi.org/10.1007/978-94-009-0067-7_13
- [7] Zhang, F., Wu, X., Zhou, W., et al. (2019) Study on the Compatibility of Multi-Bifurcations by Simulations of Pattern Formation. *IEEE Access*, **7**, 186538-186552. <https://doi.org/10.1109/ACCESS.2019.2959944>

-
- [8] Zhang, F., Zhang, H., Evans, M.R., *et al.* (2017) Vegetation Patterns Generated by a Wind Driven Sand-Vegetation System in Arid and Semi-Arid Areas. *Ecological Complexity*, **31**, 21-33. <https://doi.org/10.1016/j.ecocom.2017.02.005>
- [9] Guckenheimer, J. and Holmes, P. (1993) Nonlinear Oscillations, Dynamical Systems, and Bifurcations of Vector Fields. *Physics Today*, **38**, 102-105. <https://doi.org/10.1063/1.2814774>
- [10] Wen, G.L. (2005) Criterion to Identify Hopf Bifurcations in Maps of Arbitrary Dimension. *Physical Review E Statistical Nonlinear & Soft Matter Physics*, **72**, Article ID 026201. <https://doi.org/10.1103/PhysRevE.72.026201>
- [11] Wang, Q., Fan, M. and Wang, K. (2003) Dynamics of a Class of Nonautonomous Semi-Ratio-Dependent Predator-Prey Systems with Functional Responses. *Journal of Mathematical Analysis & Applications*, **278**, 443-471. [https://doi.org/10.1016/S0022-247X\(02\)00718-7](https://doi.org/10.1016/S0022-247X(02)00718-7)
- [12] Guill, C., Reichardt, B., Drossel, B., *et al.* (2011) Coexisting Patterns of Population Oscillations: The Degenerate Neimark-Sacker Bifurcation as a Generic Mechanism. *Physical Review E Statistical Nonlinear & Soft Matter Physics*, **83**, 021910. <https://doi.org/10.1103/PhysRevE.83.021910>
- [13] Qamar, D., Elsadany, A.A. and Hammad, K. (2017) Neimark-Sacker Bifurcation and Chaos Control in a Fractional-Order Plant-Herbivore Model. *Discrete Dynamics in Nature and Society*, **2017**, Article ID 6312964. <https://doi.org/10.1155/2017/6312964>
- [14] Tanaka, G., Tsumoto, K., Tsuji, S., *et al.* (2008) Bifurcation Analysis on a Hybrid Systems Model of Intermittent Hormonal Therapy for Prostate Cancer. *Physica D Nonlinear Phenomena*, **237**, 2616-2627. <https://doi.org/10.1016/j.physd.2008.03.044>